

The Enigmatic Radio Afterglow of GRB 991216

D. A. Frail¹, E. Berger², T. Galama², S. R. Kulkarni², G. H. Moriarty-Schieven³, G. G. Pooley⁴, R. Sari⁵, D. S. Shepherd¹, G. B. Taylor¹, F. Walter²

ABSTRACT

We present wide-band radio observations spanning from 1.4 GHz to 350 GHz of the afterglow of GRB 991216, taken from 1 to 80 days after the burst. The optical and X-ray afterglow of this burst were fairly typical and are explained by a jet fireball. In contrast, the radio afterglow is unusual in two respects: (a) the radio light curve does not show the usual rise to maximum flux on timescales of weeks and instead appears to be declining already on day 1 and (b) the power law indices show significant steepening from the radio through the X-ray bands. We show that the standard fireball model, in which the afterglow is from a forward shock, is unable to account for (b) and we conclude that the bulk of the radio emission must arise from a different source. We consider two models, neither of which can be ruled out with the existing data. In the first (conventional) model, the early radio emission is attributed to emission from the reverse shock as in the case of GRB 990123. We predict that the prompt optical emission would have been as bright (or brighter) than 8th magnitude. In the second (exotic) model, the radio emission originates from the forward shock of an isotropically energetic fireball (10^{54} erg) expanding into a tenuous medium (10^{-4} cm⁻³). The resulting fireball would remain relativistic for months and is potentially resolvable with VLBI techniques. Finally, we note that the near-IR bump of the afterglow is similar to that seen in GRB 971214 and no fireball model can explain this bump.

Subject headings: gamma rays:bursts – radio continuum:general – cosmology:observations

¹National Radio Astronomy Observatory, P. O. Box O, Socorro, NM 87801

²California Institute of Technology, Owens Valley Radio Observatory 105-24, Pasadena, CA 91125

³Joint Astronomy Centre, 600 A'Ohoku Place, Hilo, HI 96720

⁴Mullard Radio Astronomy Observatory, Cavendish Laboratory, Madingley Road, Cambridge CB3 0HE

⁵California Institute of Technology, Theoretical Astrophysics 103-33, Pasadena, CA 91125

1. Introduction

The intense gamma-ray burst GRB 991216 was detected on 1999 December 16.67 UT by the Burst and Transient Experiment (BATSE) on board the *Compton Gamma Ray Observatory* satellite (Kippen, Preece & Giblin 1999). Follow-up observations with the PCA instrument on the *Rossi X-ray Timing Explorer* (RXTE) satellite resulted in the detection of a previously uncataloged X-ray source, which was subsequently seen to fade by a factor of five, seven hours later (Takeshima *et al.* 1999). Uglesich *et al.* (1999) identified a fading optical source, at a position consistent with the RXTE transient, and shortly thereafter the radio counterpart was discovered (Taylor & Berger 1999).

Here we present radio measurements of this burst from 1 GHz to 350 GHz. While the emission from X-ray and optical afterglow was fairly typical (Halpern *et al.* 2000), the radio afterglow of GRB 991216 was unusual in two respects. First, the onset of the decay began much earlier than that in most radio afterglows. Second, the temporal decay indices in the radio, optical and X-ray bands are markedly different from each other. We explore a number of possible explanations for these behaviors.

2. Observations

*Very Large Array (VLA)*⁶: A log of the observations and flux density measurements are summarized in Table 1. We used J0509+1011 (at 8.46 GHz and 4.86 GHz) and J0530+135 (at 1.43 GHz) for phase calibration. J0542+498 was used for flux calibration at all frequencies.

*Very Long Baseline Array (VLBA)*⁶: A single 2-hr observation was carried out at 8.42 GHz and 2-bit samples of a 64 MHz bandwidth signal in one hand of polarization were recorded. The nearby ($< 1.1^\circ$) calibrator J0509+1011, a core-jet source, was observed every 3 minutes for delay, fringe rate and fringe phase calibration. The total flux density of the calibrator was found to be 9.5% less than was measured by the VLA on the same day. Given that the jet of J0509+1011 is likely to have some extended emission that is not detectable by the VLBA, it is likely that the absolute flux calibration of the VLBA is well within its nominal value of 5%.

The radio afterglow was detected at a position of (epoch J2000) $\alpha = 5^h 9^m 31.2983^s$,

⁶The NRAO is a facility of the National Science Foundation operated under cooperative agreement by Associated Universities, Inc. NRAO operates both the VLA and the VLBA.

$\delta = +11^\circ 17' 7.262''$, with (conservative $1\text{-}\sigma$ error of $0.001''$ in each coordinate). The source is unresolved with a size of less than $0.001''$.

Ryle Telescope: Observations at 15 GHz with the Ryle Telescope at Cambridge (UK) were made by interleaving 15 minute scans of GRB 991216 with short scans of the phase calibrator J0509+1011. The flux density scale was tied to observations of 3C 48 and 3C 286.

Owens Valley Radio Observatory Interferometer (OVRO): The source was observed for a single 13 hr track in two continuum 1 GHz bands (central frequencies 98.481 GHz and 101.481 GHz) under good 3-mm weather conditions. Gain calibration used the quasar 0528+134, while observations of Uranus and 3C 454.3 provided the flux density calibration scale with an estimated uncertainty of $\sim 20\%$. See Shepherd et al. (1998), for details of the calibration and imaging. No source was detected (see Table 1).

James Clark Maxwell Telescope (JCMT⁷): Observations in the 350 GHz band were made using the Sub-millimeter Common-User Bolometer Array (Holland *et al.* 1999). The data were taken under good sky conditions on both nights. For flux calibration we used the source CRL618, and assumed its flux density to be 4.57 ± 0.21 Jy. The pointing was monitored and found to vary by less than $2''$. See Kulkarni et al. (1999) for details of data reduction. The source was not detected at either epoch (see Table 1). At the position of GRB 991216 we derive an average flux of -0.28 ± 1.1 mJy.

3. Results

In Figure 1 we display the 8.46 GHz light curve, as well as the X-ray and optical (R-band) light curves obtained from measurements reported in the GRB Coordinates Network (GCN)⁸ and Halpern et al. (2000). A noise-weighted least squares fit of the form $F_\nu \propto t^{\alpha_\nu}$ was made to each of these light curves. Using all the 8.46 GHz data, including the upper limits, we derive $\alpha_r = -0.82 \pm 0.02$ ($\chi_r^2 = 26.5/15$; here χ_r^2 is the reduced χ^2).

A similar least squares fit of the optical and X-ray data over the first three days (Figure 1), yields $\alpha_o = -1.33 \pm 0.01$ ($\chi_r^2 = 11/28$) and $\alpha_x = -1.61 \pm 0.06$ ($\chi_r^2 = 7.7/3$). From a more extensive dataset, Halpern et al. (2000) fit $\alpha_o = -1.07_{-0.08}^{+0.17}$ over the same time range. We will use their value of α_o in the discussion to follow. The relatively large value of χ_r^2 for

⁷The JCMT is operated by The Joint Astronomy Centre on behalf of the Particle Physics and Astronomy Research Council of the UK, the Netherlands Organization for Scientific Research, and the National Research Council of Canada.

⁸http://lheawww.gsfc.nasa.gov/docs/gamcosray/legr/bacodine/gcn_main.html.

fit to the X-ray data presumably reflects the uncertainties inherent in converting the counts measured by three different instruments (RXTE-ASM, RXTE-PCA and Chandra ACIS) into Jansky flux units. Using the RXTE-PCA data alone avoids this cross-calibration issue and yields $\alpha_x = -1.61 \pm 0.05$.

4. The Unusual Nature of the Radio Afterglow: The Failure of the Basic Afterglow Model

The radio afterglow from GRB 991216 is unusual on two counts. First, the radio afterglow in the centimeter band does not show the usual rise to a peak value f_m (at epoch t_m) before undergoing a power law decay. The radio flux appears to decline continuously starting from the epoch of the first observation. Thus $t_m < 1.49$ d as compared to the 10–100 d seen in other bursts (e.g. Frail, Waxman & Kulkarni 2000, Frail *et al.* 1999, Frail *et al.* 1999). Second, the temporal decay indices (α_ν) in the radio, optical and X-ray bands are markedly different from each other. Proceeding from radio to higher frequencies, α_ν steepens by ~ 0.4 every four decades in frequency.

In contrast, the optical and X-ray afterglow appears to find a straightforward explanation in the standard afterglow model in which a jet geometry is invoked (Halpern *et al.* 2000). Below we show that the radio observations cannot be reconciled with a standard jet (or sphere) afterglow model. We then explore possible modifications to the standard model.

The simplest afterglow model is one in which the broad-band afterglow emission arises from the forward shock of a relativistic blast wave propagating into a constant density medium (Sari, Piran & Narayan 1998). It is assumed that the electrons in the forward shock region are accelerated to a power law distribution for $\gamma_e > \gamma_m$, $dN/d\gamma_e \propto \gamma_e^{-p}$; here γ_e is the Lorentz factor of the electrons, p is the power law index and γ_m is the minimum Lorentz factor. Gyration of these electrons in strong post-shocked magnetic fields gives rise to broad-band afterglow emission. Two modifications to this picture are routinely considered. (1) An inhomogeneous circumburst medium (specifically, $\rho(r) \propto r^{-2}$; here ρ is the density at distance r from the source). Such a circumburst medium is expected should GRBs originate from massive stars (Chevalier & Li 1999). (2) A jet-like geometry for the blast wave (Sari, Piran & Halpern 1999). This modification is motivated by the propensity of jets in astrophysical sources.

Regardless of these modifications, the broad band spectrum is composed of three characteristic frequencies: ν_a , the synchrotron self-absorption frequency; ν_m , the frequency

at which the emission peaks (and attributed to the electrons with Lorentz factor γ_m), and ν_c , the cooling frequency. Electrons radiating photons with frequency $> \nu_c$ cool on timescales faster than the age of the blast wave. The evolution of these frequencies is determined by the dynamics of the blast wave. The usual ordering of these frequencies at epochs relevant to the discussion here is (going from low to high frequencies) ν_a , ν_m and ν_c .

For GRB 991216 the early radio decay implies that ν_m is already below the centimeter radio band at 1.49 days. The steepening of the afterglow emission from optical to X-ray can be explained by placing ν_c between the optical and X-ray bands. The expected steepening $\Delta\alpha$ is 1/4 which is marginally consistent with $\alpha_o - \alpha_x = 0.54^{+0.18}_{-0.10}$. However, even if we ignore this, we are simply unable to explain the decay in the radio band, since no additional steepening is expected between ν_m and ν_c .

The standard afterglow model can be made to agree with the light curves by postulating an energy slope p which gradually steepens with increasing electron energy γ_e . We use the spherical, constant density afterglow model (Sari, Piran & Narayan 1998) to convert, in each band, the observed decay index to p and obtain: $p = 2.09 \pm 0.03$ (radio), $p = 2.43^{+0.23}_{-0.11}$ (optical), and $p = 2.81 \pm 0.08$ (if ν_c is below the X-ray band) or $p = 3.15$ (if ν_c above the X-ray band). We are justified in applying the spherical model for early times ($t < t_J \sim 2\text{--}5$ d) since the jet geometry is manifested only for $t > t_J$ (Halpern *et al.* 2000).

Curvature is both observed and modeled in the synchrotron spectra of the non-relativistic shocks from supernova remnants which are accelerating cosmic rays (e.g. Baring *et al.* 1999). To date, models of ultra-relativistic shocks favor a universal value of p , independent of energy (Vietri 2000, Gallant *et al.* 2000), but non-linear effects have yet to be treated.

Nonetheless, the invocation of curvature in the energy distribution of the electrons cannot explain the observed broad-band spectrum (Figure 2) of the afterglow on December 18 (corresponding to 1.33 days after the burst). A plausible fit to the entire data is obtained with $\nu_a = 1.3$ GHz, $\nu_m = 270$ GHz and $\nu_c = 7 \times 10^{16}$ Hz and $f_m = 3.4$ mJy; this fit is displayed by the dashed line in Figure 2. As the blast wave slows down, ν_m moves to lower values while preserving f_m and thus we expect the flux in the centimeter band to rise, whereas the observed flux falls. If the afterglow has a jet-like geometry then the radio afterglow is expected to rise until the epoch t_J , and subsequently decay very slowly ($f_\nu \propto t^{-1/3}$) until ν_m passes through the centimeter band, after which we expect to see a decline similar to that seen in the optical ($f_\nu \propto t^{-2.2}$) (Harrison *et al.* 1999). As can be seen from Figure 2, the radio observations are grossly inconsistent with these expectations, particularly the decay is much faster than $t^{-1/3}$.

To summarize, while the optical and X-ray observations can be accounted for by a jet model, the radio observations are inconsistent with the standard model. This forces us to consider afterglow models in which the radio emission (at least in bulk) arises from a source other than the usual forward shock.

5. A Forward and Reverse Shock Model

The most natural explanation for two components would be an early contribution from a reverse shock followed by a forward shock element at later times. This is the explanation invoked to account for the early (1-2 day) radio emission from the afterglow of GRB 990123 (Sari & Piran 1999, Kulkarni *et al.* 1999 but see Galama *et al.* 1999). The two bursts share several common features: in both cases, a jet has been deduced with $t_J \sim$ few days, both were quite bright at gamma-ray energies and finally both had a seemingly small value of t_m (as measured in the centimeter band). However, in the case of GRB 990123, the peak flux of the forward shock was $f_m < 260 \mu\text{Jy}$ (Kulkarni *et al.* 1999) and the radio light curve was dominated by the reverse shock. In contrast, the forward shock for GRB 991216 appears to be quite strong. This difference then explains the seemingly different radio light curves.

At late times (i.e. timescales greater than the duration of the burst) the flux from the reverse shock is expected to fall as $t^{-1.8}$ (Kobayashi & Sari 2000). In contrast, the forward shock emission rises as $t^{1/2}$ for $t < t_J$ and then slowly decays, $\propto t^{-1/3}$ until the ν_m moves into the centimeter band. Since t_J is known from optical observations (Halpern *et al.* 2000), the remaining unknowns are the strength of the reverse and forward shock emission.

In this picture, the reverse shock dominates the radio emission for the first few days and the model fit consists of mainly fitting a power law with $f_\nu \propto t^{-1.8}$. We note that at day 1.5, the VLA 8.46 GHz flux and the Ryle 15 GHz flux are comparable. This suggests that the reverse shock is already optically thin at 8.46 GHz at this epoch – similar to the situation for GRB 990123 (Kulkarni *et al.* 1999). We deduce the parameters of the forward shock by fitting the radio to optical spectrum around $t_J=5$ days to the forward shock model (the contribution of the reverse shock is expected to be negligible thanks to the steep decay and since t is comparable to t_J , the spherical fireball model is still applicable); we find $\nu_m \sim 1.4 \times 10^{12}$ Hz and $f_m = 1$ mJy. As can be seen from Figure 3 this reverse-forward model provides a reasonable fit to the observations.

There are two predictions of this model. First, we expect ν_m to cross the centimeter band at $t_b = t_J(\nu_m/8.46 \text{ GHz})^{1/2} \sim 64$ d. For $t > t_b$, we expect the radio flux to decline as steeply as the optical flux does for $t > t_J$. The low flux values as measured at the VLA

around this epoch are in agreement with this model.

A second prediction is that for $t < t_b$, we expect, the spectrum to rise as $\nu^{1/3}$ for $\nu < 8.46$ GHz. Unfortunately, the data are too sparse to rigorously test this expectation. Nonetheless, we note that at day 17.44, the spectrum between 1.43 and 8.46 GHz can be described by a simple power-law with slope $\beta_r = -0.45$, steeper than a $\nu^{1/3}$ slope by 3.6σ . We consider this to be the weakest point of the model but do not consider it fatal since the quoted uncertainties include only instrumental errors and do not include external effects such as interstellar scintillation.

The strongest confirmation of this model would have been the detection of an optical flash, as in the case of GRB 990123 (Akerlof *et al.* 1999). The strong radio emission from the reverse shock allows us to predict (by scaling from the optical and radio observations of GRB 990123, Sari & Piran 1999) that the flash would have been 8th magnitude or even brighter. Unfortunately, this event occurred during daytime and therefore was not observed by existing prompt optical counterpart experiments (LOTIS – H. S. Park; ROSTE – C. Akerlof; *pers. comm.*)

We end this section by noting a worrisome and puzzling issue: we are unable to provide a consistent explanation for the near-IR, optical and X-ray observations with a standard fireball afterglow spectrum. As noted in Figure 2, there is a broad maximum around 2×10^{14} Hz – suggesting that this is the peak frequency (ν_m) of the fireball. Fitting a template afterglow spectrum we obtain the following: $\nu_{m1} = 2.1 \pm 0.6 \times 10^{14}$ Hz, $f_{m1} = 150 \pm 10 \mu\text{Jy}$ and $\nu_{c1} = 2 \times 10^{16}$ Hz. We note that a similar broad peak in the near IR (and attributed to $\nu_m \sim 3 \times 10^{14}$ Hz at $\Delta t = 0.5$ d) was observed for GRB 971214 (Ramaprakash *et al.* 1998). However, if we evolve this ν_m back in time (with $\nu_m \propto t^{-3.2}$) we predict a *rising* R-band light curve, inconsistent with the observations (Figure 1). Moving ν_m to lower frequencies solves this problem but we are left with no explanation for the “near-IR” bump.

6. A Two-Component Forward Shock Model

We now consider a model in which much of the radio emission arises as the forward shock of an additional fireball (hereafter the second fireball). The principal attraction of the second fireball is that we no longer need to relate the radio decay rate to those at optical and radio frequencies. We clarify that the optical and X-ray observations are explained by the forward shock of the fireball (the first fireball) discussed in the previous section. As noted earlier, there is good evidence suggesting that the first fireball is a jet. Thus the second fireball must be a more isotropic fireball and move at a smaller Lorentz factor.

Indeed, in some GRB models, the central engine is expected to inject two fireballs: a high Γ jet and a low Γ spherical wind.

A reasonable fit to the radio data of this second fireball (FS 2; see Figure 2) on day 1.33 is provided by $f_{m2} \simeq 1.2$ mJy, $\nu_{m2}=7$ GHz, and $\nu_{a2}=2$ GHz. The location of the cooling frequency ν_{c2} is unconstrained. As a test, we evolved the afterglow spectrum forward in time. The model does an excellent job reproducing the declining flux density from 1.43 and 8.46 GHz at 17.44 days (an observation which the reverse-forward shock model fails to explain), but at day 60.40 it predicts a 1.43 GHz flux of ~ 100 μ Jy, where only an upper limit of -57 ± 44 μ Jy is measured. Again we consider this $3\text{-}\sigma$ discrepancy as a major, but not fatal, weakness of this model.

The three inferred parameters (ν_{m2} , f_{m2} , ν_{a2}) allow us to obtain the energy of the blast wave and the density of the ambient medium (Wijers & Galama 1999): $E_{52} \sim 10^2$ erg and $n \sim 10^{-4}$ cm^{-3} ; these values are relatively insensitive to the value of the unknown ν_c (which is however constrained to lie above the optical band). The large E and small n are primarily due to the small value of t_m .

If this interpretation is correct then we have uncovered the first example of a GRB exploding in a very low density medium – perhaps the halo of a host galaxy. The dynamics of explosions is governed by the ratio E/n , and as noted above, this ratio is perhaps 10^5 larger than that typically derived in other afterglow. For this reason, both fireballs, the high Γ and the low Γ fireballs, would then be expanding at high Lorentz factors days after the burst. The Γ for the low Γ fireball would be an impressive 20 one day after the burst, and the fireball would have had a size of 100 microarcseconds three weeks after the burst – almost within reach of measurable with VLBI techniques (cf. Taylor *et al.* 1997). The jet fireball would be expanding even faster in which case the opening angle of the jet is not 6° (Halpern *et al.* 2000) but only 1° .

To summarize, the radio afterglow of GRB 991216 is unusual and cannot be explained by the standard forward shock model. A conventional reverse-forward shock model or an exotic two-component forward shock model can account for the observations, but each has one major (but not necessarily fatal) weakness. Finally, we have no explanation for the near-IR bump seen on day 1.33. GRB 991216 shows that there may be yet new surprises in GRB afterglows.

DAF thanks Chris Fassnacht, Steve Myers, Lin Yan and Jim Ulvestad for generously giving up portions of their VLA time so that GRB 991216 could be observed. DAF thanks J. Halpern for making his paper available prior to publication and Y. Gallant and M. Vietri for useful discussions. We would like to thank S. Jogiee for preparing the first observations

of this burst at the Owens Valley Observatory and A. Sargent for generously allocating the time on short notice. Research at the Owens Valley Radio Observatory is supported by the National Science Foundation through NSF grant number AST 96-13717. SRK's research is supported by grants from NSF and NASA. RS and TJG are supported by Sherman Fairchild Fellowships.

REFERENCES

- Akerlof, C. *et al.* 1999, *Nature*, 398, 400.
- Baring, M. G., Ellison, D. C., Reynolds, S. P., Grenier, I. A., and Goret, P. 1999, *ApJ*, 513, 311.
- Chevalier, R. A. and Li, Z.-Y. 1999, *ApJ* (Let) submitted;astro-ph/9908272.
- Corbet, R. and Smith, D. 1999, GCN notice 506.
- Frail, D. *et al.* 1999, *ApJ*. *ApJ* submitted; astro-ph/9910060.
- Frail, D. A. *et al.* 1999, *ApJ* (Let) in press; astro-ph/9909407.
- Frail, D. A., Waxman, E., and Kulkarni, S. R. 2000, *ApJ* in press; astro-ph/9910319.
- Fukugita, M., Shimasaku, K., and Ichikawa, T. 1995, *PASP*, 107, 945.
- Galama, T. J. *et al.* 1999, *Nature*, 398, 394.
- Gallant, Y. A., Achterberg, A., Kirk, J. G., and Guthmann, A. W. 2000, 5th Huntsville Gamma-Ray Burst Symposium, in press, astro-ph/0001509.
- Granot, J., Piran, T., and Sari, R. 1999a, *ApJ*, 513, 679.
- Granot, J., Piran, T., and Sari, R. 1999b, *ApJ* in press; astro-ph/9908007.
- Halpern, J. P., Uglesich, R., Mirabal, N., Kassin, S., *et al.* 2000, *ApJ* (Let) submitted.
- Harrison, F. A. *et al.* 1999, *ApJ*, 523, L121.
- Holland, W. S. *et al.* 1999, *mnras*, 303, 659.
- Kippen, R. M., Preece, R. D., and Giblin, T. 1999, GCN notice 463.
- Kobayashi, S. and Sari, R. 2000, astro-ph/9910241.
- Kulkarni, S. R. *et al.* 1999, *ApJ*, 522, L97.
- Piro, L., Garmire, G., Garcia, M., Marshall, F., and Takeshima, T. 1999, GCN notice 500.
- Ramaprakash, A. N. *et al.* 1998, *Nature*, 393, 43.
- Rol, E., Vreeswijk, P. M., Strom, R., Kouveliotou, C., Pian, E., Castro-Tirado, A., Hjorth, J., and Greiner, J. 1999, GCN notice 491.

- Sari, R. and Piran, T. 1999, ApJ, 517, L109.
- Sari, R., Piran, T., and Halpern, J. P. 1999, ApJ, 519, L17.
- Sari, R., Piran, T., and Narayan, R. 1998, ApJ, 497, L17.
- Schlegel, D. J., Finkbeiner, D. P., and Davis, M. 1998, ApJ, 500, 525.
- Shepherd, D. S., Frail, D. A., Kulkarni, S. R., and Metzger, M. R. 1998, ApJ, 497, 859.
- Takeshima, T., Markwardt, C., Marshall, F., GIBLIN, T., and KIPPEN, R. M. 1999, GCN notice 478.
- Taylor, G. B. and Berger, E. 1999, GCN notice 483.
- Taylor, G. B., Frail, D. A., Beasley, A. J., and Kulkarni, S. R. 1997, Nature, 389, 263.
- Uglesich, R., Mirabal, N., Halpern, J., Kassin, S., and Novati, S. 1999, GCN notice 472.
- Vietri, M. 2000, ApJ (Let) submitted, astro-ph/0002269.
- Wijers, R. A. M. J. and Galama, T. J. 1999, ApJ, 523, 177.

Table 1. Radio Observations of GRB 991216

Epoch (UT)	Δt (days)	Telescope	ν_o (GHz)	$S \pm \sigma$ (μJy)
1999 Dec. 18.00	1.33	Ryle	15.0	1100±250
1999 Dec. 18.16	1.49	VLA	8.46	960±67
1999 Dec. 18.32	1.65	VLBA	8.42	705±85
1999 Dec. 18.48	1.81	JCMT	350	650±1560
1999 Dec. 19.30	2.63	OVRO	99.9	90±700
1999 Dec. 19.35	2.68	VLA	8.46	607±32
1999 Dec. 19.45	2.78	JCMT	350	−2000±1670
1999 Dec. 20.09	3.42	Ryle	15.0	−100±400
1999 Dec. 22.01	5.34	Ryle	15.0	−10±200
1999 Dec. 23.30	6.63	VLA	8.46	343±43
1999 Dec. 24.29	7.62	VLA	8.46	127±58
1999 Dec. 26.40	9.73	VLA	8.46	170±72
1999 Dec. 28.24	11.57	VLA	8.46	211±25
1999 Dec. 29.43	12.76	VLA	8.46	136±37
1999 Dec. 31.26	14.59	VLA	8.46	123±39
2000 Jan. 2.01	16.34	VLA	8.46	130±22
2000 Jan. 3.11	17.44	VLA	8.46	131±36
2000 Jan. 3.11	17.44	VLA	4.86	126±31
2000 Jan. 3.11	17.44	VLA	1.43	257±51
2000 Jan. 6.15	20.48	VLA	8.46	123±30
2000 Jan. 23.95	38.28	VLA	8.46	79±31
2000 Jan. 28.16	42.49	VLA	8.46	148±33
2000 Feb. 05.18	50.51	VLA	8.46	3.1±30
2000 Feb. 15.07	60.40	VLA	1.43	−57±44
2000 Feb. 15.07	60.40	VLA	8.46	9.6±24
2000 Mar. 03.85	78.18	VLA	8.46	47.0±19

Note. — The columns are (left to right), (1) UT date of the start of each observation, (2) time elapsed since the GRB 991216 event (i.e. $t_o=1999$ December 16.67 UT), (3) telescope name, (4) observing frequency, (5) flux density of the radio transient, with the error given as the rms noise on the image. The epoch on Jan. 23.95 UT is an average of two days of data (Jan. 21.95 UT and Jan. 25.94 UT). All VLA observations were made when it was in its “B-array” configuration.

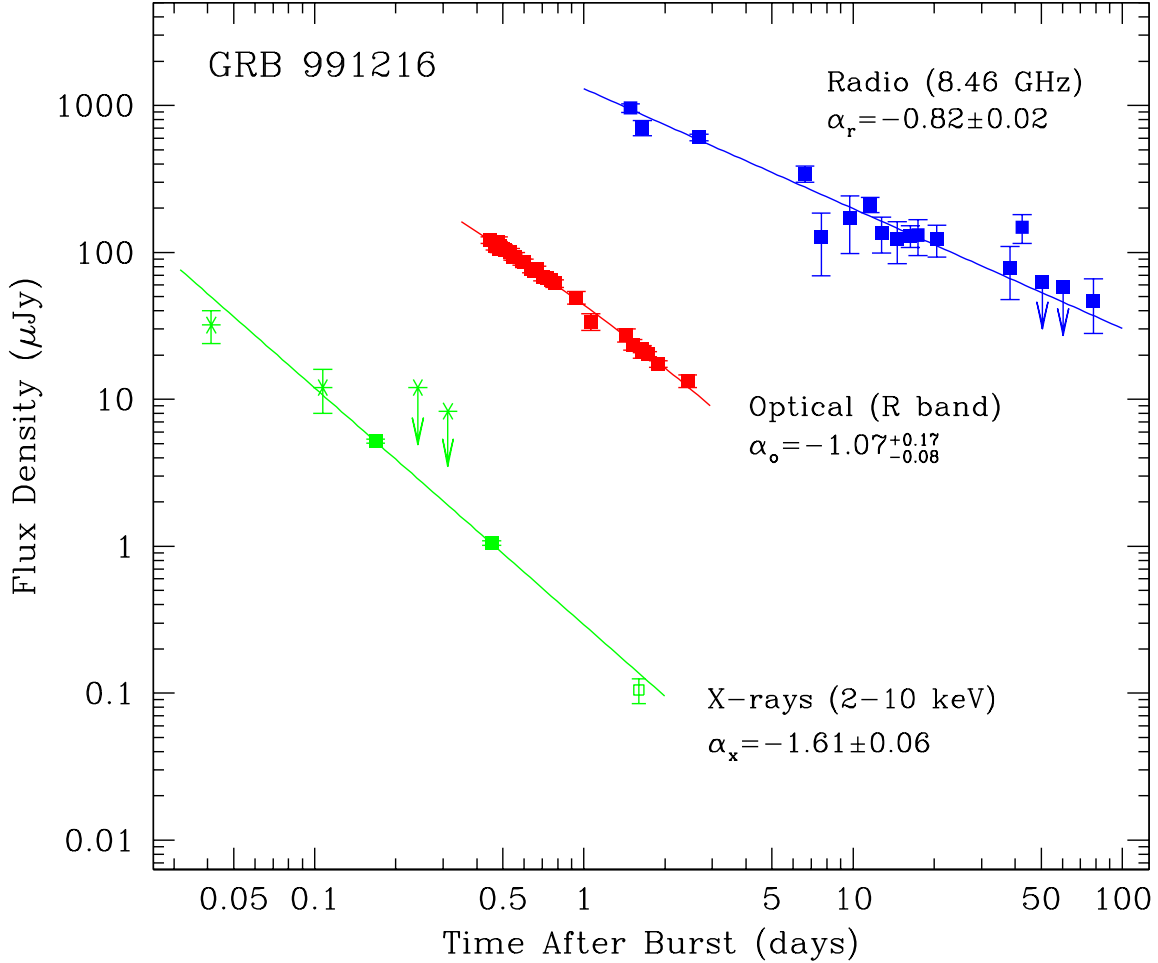


Fig. 1.— Broad-band light curves of GRB 991216. Upper limits are plotted as the peak flux density at the location of the afterglow plus two times the rms noise in the image. The R-band data are taken from Halpern *et al.* (2000). Optical magnitudes were converted to Jansky flux units (Fukugita, Shimasaku & Ichikawa 1995) but no correction has been made for Galactic extinction. The X-ray data are measurements taken by the ASM (*) and PCA (filled squares) instruments on RXTE (Corbet & Smith 1999, Takeshima *et al.* 1999), and the Chandra X-ray Observatory (\square ; Piro *et al.* 1999). X-ray fluxes are converted to Janskys using the X-ray slope $\beta_x = -1.1$ derived by Takeshima *et al.* (1999). The solid lines are noise-weighted least squares fits to the data, with the slopes α_ν as indicated (see text for details).

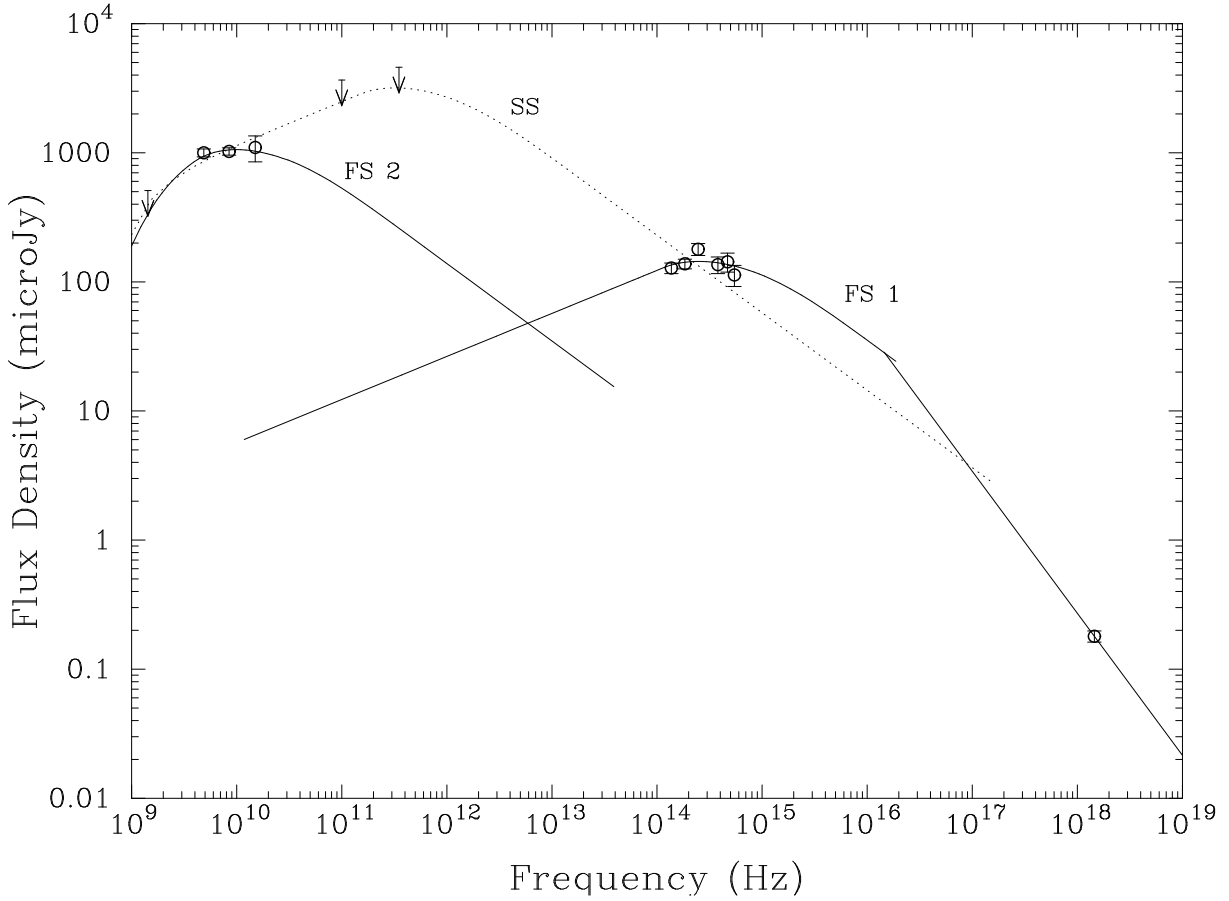


Fig. 2.— Radio to X-ray spectral flux distribution of GRB 991216 on 1999 December 18.00 ($\Delta t=1.33$ days after the burst). Optical and infrared measurements are taken from Halpern et al. (2000) and are interpolated to this epoch assuming the decay rate of $\alpha_o = -1.07_{-0.08}^{+0.17}$, as measured by Halpern et al. at early times. The optical/IR data have been corrected for Galactic foreground extinction (Schlegel, Finkbeiner & Davis 1998), giving $E(B-V)=0.634$ with an uncertainty of 10%. The 1.4 GHz upper limit (plotted as three times the rms noise) and the 4.8 GHz data point were taken at the Westerbork Synthesis Radio Telescope (WSRT) by Rol et al. (1999). The flux density at 8.46 GHz derived by extrapolating of the power-law decay in Figure 1. The upper limits at 100 GHz and 350 GHz have been extrapolated back to this epoch by assuming a worst case decay rate of $\alpha_o - 2\sigma$. The dotted and solid lines are fits to the data for a synchrotron spectrum from a relativistic blast wave as specified by Granot et al. (1999a; see their Figure 10 for the equipartion field model). We assume $p = 2.2$ and scale it by ν_m and f_m to derive a function $g(\nu)$ with asymptotic limits of $\nu^{1/3}$ and $\nu^{(p-1)/2}$. We account for synchrotron self-absorption at ν_a by multiplying $g(\nu)$ by $F_\nu = [1 - \exp(-\tau)]/\tau$, where $\tau = (\nu/\nu_a)^{-5/3}$ (Granot, Piran & Sari 1999b).

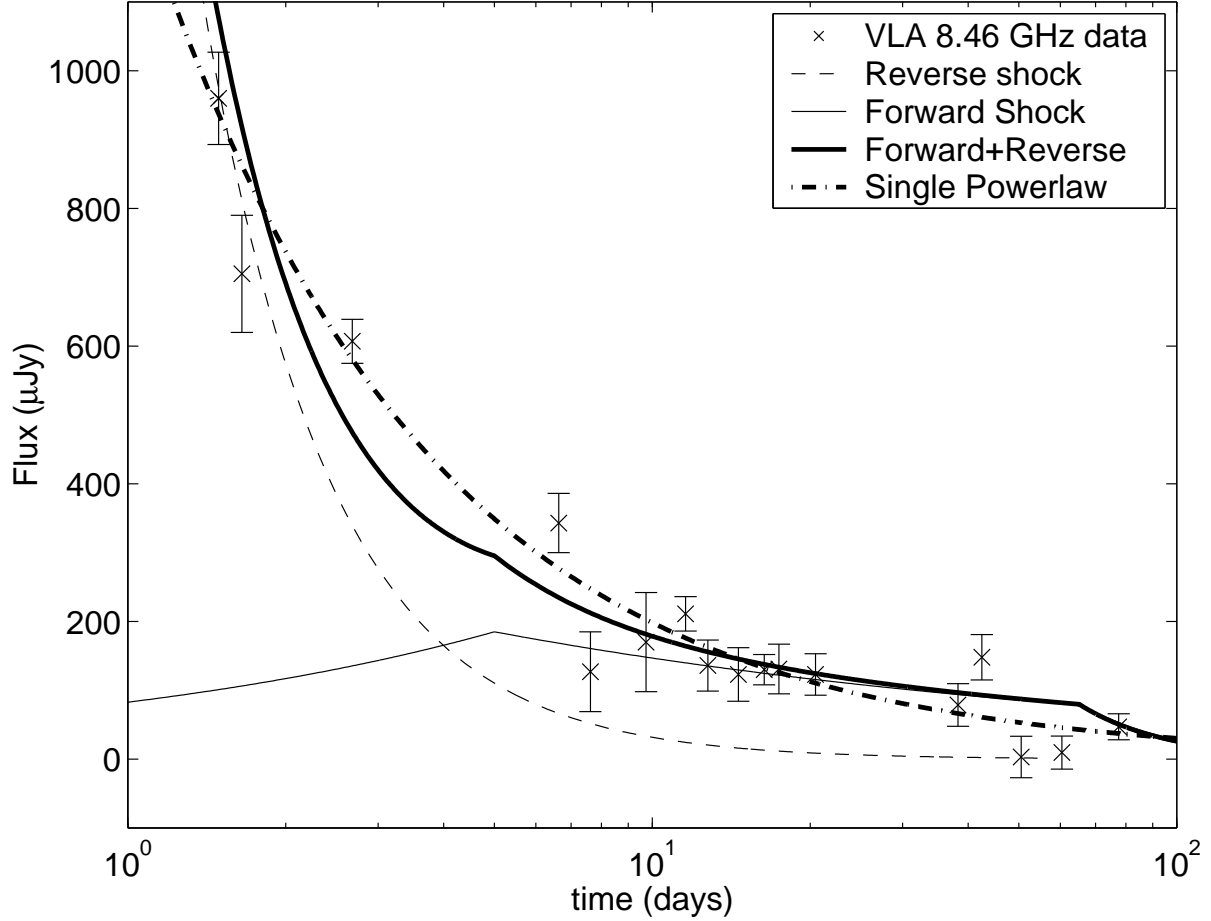


Fig. 3.— Observed and model light curves at 8.46 GHz. The dot-dashed line is the power-law fit from Figure 1. The thick solid line is the two component model discussed in §5, consisting of a reverse shock (dashed line) and a forward shock (thin solid line). See text for more details.